Diffusion of Macromolecules in Polymer Solutions and Gels: A Laser Scanning Confocal Microscopy Study

Matthew D. Burke,[†] Jung O. Park,[‡] Mohan Srinivasarao,*[,‡] and Saad A. Khan*[,†]

Department of Chemical Engineering, North Carolina State University, Raleigh, North Carolina 27695-7905, and School of Textile & Fiber Engineering, Georgia Institute of Technology, Atlanta, Georgia 30332-0295

Received May 5, 2000; Revised Manuscript Received July 24, 2000

ABSTRACT: Laser scanning confocal microscopy combined with fluorescence recovery after photobleaching is an effective tool to measure the diffusion coefficients of macromolecules in cross-linked hydrogels and polymer solutions. In this study, the effects of enzyme treatment on the diffusion of macromolecules (FITC-dextran) in guar solutions and titanium-guar hydrogels are examined. Enzyme treatment with β-mannanase, a polymer backbone cleaving enzyme, quickly increases the diffusion coefficient of the probe molecules in both solutions and hydrogels to that in water. Enzyme treatment of guar solutions and hydrogels with α-galactosidase, a side chain cleaving enzyme, displays a unique behavior due to changes in the fine structure of guar. The removal of galactose branches from the mannan backbone of guar creates additional hyperentanglements (i.e., cross-links), which reduce the water holding capacity of guar and induce syneresis. If the depth at which the diffusion coefficient is measured remains constant, a minimum is observed in the diffusion coefficient as α-galactosidase enzyme treatment time increases. At the site of measurement, the sample changes from a homogeneous guar system to a phase-separated polymer-rich hydrogel and finally to a dilute polymer phase as the polymer-rich hydrogel phase precipitates below the site of measurement. The diffusion coefficient in the dilute polymer phase increases to that in water, while the diffusion coefficient in the hydrogel phase continues to decrease to a value of approximately 6×10^{-8} cm^2/s.

I. Introduction

Guar galactomannan solutions and hydrogels are used extensively in a range of applications from the petroleum to textile and food industries because of their natural abundance (second only to cellulose), biodegradability, low cost, and unique ability to alter rheological properties.[1−3] For many of these uses, enzymes offer a powerful tool to modify the biopolymer microstructure to develop galactomannans with tailored rheological properties and novel functional performance.[4,5] However, the effect of enzyme modification alters not only the rheological properties of guar but also the diffusion of macromolecules in these systems. An understanding of the diffusion properties in modified guar is essential to optimize enzyme modification conditions and ensure proper biopolymer structural features for a particular application.

While considerable work has been done to characterize guar galactomannans,[6−8] studies on diffusion in enzymatically modified galactomannan systems have never been undertaken, to the best of our knowledge. An insight into this area is critical for a variety of reasons. For example, in the petroleum industry, guar is used to entrap and transport sand particles to a desired location.[9] Premature enzyme modification of guar could increase the diffusion coefficient of these solutes and result in their release from the guar matrix during transport. A similar situation can occur in the pharmaceutical industry where guar galactomannan hydrogels are used for site-specific drug delivery.[10] Understanding the enzyme degradation and drug diffusion out of the guar matrix is essential to produce the proper drug dosage to be delivered in a specific time frame. In addition, in the food industry, blends of enzyme modified guar galactomannan with other polysaccharides are used as food additives to impart appropriate texture and functional performance for a product.[5,11] One detrimental effect that can be observed is syneresis, or phase separation, which is undesirable in food products.[12] Proper enzyme treatment conditions are required to prevent such an event from occurring. Finally, it is essential to determine how galactomannan microstructure and extent of its modification affect the enzyme mobility. A starting point to understand all such issues involves investigating the diffusion of probe (model) molecules in modified guar galactomannan, which forms the basis of this work.

Guar is a natural polysaccharide consisting of a main chain of β-(1→4) linked mannose with single unit α-(1→6) linked galactose branches.[13] Two commercially available enzymes that are commonly used to modify guar are β-mannanase and α-galactosidase. β-Mannanase cleaves the glycosidic bond between adjacent mannose sugars in the backbone of guar, while α-galactosidase cleaves the galactose branches from guar.[14] β-Mannanase is commonly used to decrease the viscosity of guar solutions, and α-galactosidase has been used to reduce the number of galactose branches to mimic the structure of other galactomannans such as locust bean gum.[5,15] Rheology is used to investigate the macroscopic properties of guar which has been enzymatically modified by both β-mannanase and α-galactosidase. However, we are unaware of reports that investigate the effect of enzyme modification on diffusion in guar solutions and hydrogels.

[†] North Carolina State University.
[‡] Georgia Institute of Technology.
* Corresponding authors. Saad A. Khan: Ph (919) 515-4519; Fax (919) 515-3465; e-mail khan@eos.ncsu.edu. Mohan Srinivasarao: Ph (404) 894-9348; Fax (404) 894-9766; e-mail mohan@tfe.gatech.edu.

10.1021/ma000786l CCC: $19.00
Published on Web 09/14/2000

Recently, the technique of fluorescence recovery after photobleaching (FRAP) has been refined through the use of a laser scanning confocal microscope (LSCM).[16] The obvious advantage of using a LSCM to perform FRAP experiments is the additional ability to visualize the sample during the experiment. In contrast to a conventional light microscope which bathes the sample in light and is viewed with the eye, a LSCM scans the sample with a focused beam of laser light, and the fluorescence emitted from the sample is detected by a photomultiplier tube detector.[17] The output is then built into an image by the computer. These images provide additional information about the quality of the experiment and prevent interference from out-of-focus fluorescence.[18]

LSCM-FRAP is a noninvasive technique based on irreversibly bleaching a fluorescent probe in a well-defined volume element with a high-intensity laser. Subsequently, the recovery of fluorescence is quantified with a low-intensity laser as unbleached fluorescent probes diffuse into the volume element.[19] LSCM-FRAP is a relatively new technique and is quickly gaining support for the quantification of diffusion coefficients in polymer gels and viscous solutions.[19−21] A recent review of diffusion in polymer gels does not include LSCM-FRAP, but it does provide an overview of alternative existing techniques.[22]

In this paper, we use the LSCM-FRAP technique to study the diffusion of fluorescently tagged dextran probes in guar galactomannan solutions and hydrogels. In addition, we modify the microstructure of guar in these systems, by using enzymes to cleave either the polymer backbone or the polymer side chains, in an effort to understand how these fundamental microstructural changes correlate with the diffusion of macromolecules.

II. Experimental Methods

Guar Solution Preparation. Glycine and sodium azide were purchased from Sigma and used as received. Guar gum, purchased from Aldrich, was sprinkled slowly into the vortex of water to a concentration of 7 mg/mL. This solution was vigorously mixed for 1 h followed by low shear mixing for 24 h. The solution was then centrifuged at 7000 rpm for 30 min. The supernatant was collected, and two volumes of ethanol were added. The precipitate was collected and lyophilized for 48 h. The purified guar was ground to a fine powder with a mortar and pestle and redissolved in deionized H_2O to the appropriate concentration. Sodium azide at 0.2 mg/mL was added as a biocide, 20 mM glycine was added, and the pH was adjusted to 9.

Preparation of Titanium-Guar Hydrogels. Hydrogels were formed by mixing a purified guar solution (prepared as mentioned above) and Tyzor 131 (titanium cross-linker) to yield a guar hydrogel. The final concentration of the guar was invariably 5 mg/mL; however, the titanium concentration varied from 0 to 0.5 mg/mL as appropriate. Tyzor 131 was a gift from Dupont Performance Chemicals and is a chelate of titanium used to cross-link aqueous polymer solutions. Guar-titanium hydrogels were synthesized on microscope slides with an incubation chamber placed over the hydrogel immediately after mixing the guar and titanium solutions. The cross-linking reaction proceeds quickly, and to ensure complete cross-linking, the gels were not disturbed for 24 h. The LSCM sample preparation is described below.

Fluorescent Probes. Fluorescein isothiocyanate dextran (FITC-dextran) probes were purchased from Sigma of molecular weights 20, 40, and 70.5 kDa. The wavelength of absorption maxima (λ_{abs}) and emission maxima (λ_{emis}) for the FITC-dextran probes were 492 and 518 nm, respectively. Excitation was conducted at 488 nm, and total emissions was collected from 515 to 670 nm. Except where noted, the concentration of the FITC-dextran probe was 0.4 mg/mL, as determined from the linear region of fluorescence intensity versus FITC-dextran probe concentration plot.

Laser Scanning Confocal Microscope Sample Preparation. Guar solutions were mixed with the appropriate FITC-dextran probe. After placing 100 μL of this solution on an ESCO frosted microscope slide, a Grace Bio-Labs incubation chamber (PC200) was placed over it. The total volume of the incubation chamber was 200 μL with a height of approximately 220 μm. Guar-titanium hydrogels were synthesized in the incubation chamber, and FITC-dextran probe was added after 24 h. To create a hydrogel with a homogeneous FITC-dextran concentration, the sample was then placed on a Thermolyne RotaMixer (type 48200) for 24 h at 100 rpm. Aluminum foil was placed over the sample to prevent stray light from bleaching the FITC-dextran probes.

Enzyme Degradation. *Aspergillus niger* β-mannanase (Megazyme, Ireland, Lot 50401, 41 U/mg, 297 U/mL) and guar seed α-galactosidase (Megazyme, Ireland, Lot 50701, 150 U/mL) enzymes were used without further purification. Guar solutions were prepared at a concentration of 10 mg/mL. Enzyme stock solutions were prepared at 0.2 U/mL for β-mannanase and 2 U/mL for α-galactosidase. Guar and enzyme solutions were separately preincubated at 25 °C for 15 min, followed by the addition of the appropriate amount of enzyme to the guar solution. The mixture was gently shaken at an agitation setting of 2 (approximately 80 rpm) at 25 °C for the appropriate amount of time in an New Brunswick gyrotory water bath shaker (model G76). The enzyme was denatured by placing the enzyme/guar solution in an 80 °C water bath for 10 min. Guar-titanium hydrogels were degraded in a similar fashion; however, degradation took place in the incubation chamber at room temperature (∼22 °C), and the sample was placed on the Thermolyne RotaMixer at 100 rpm for the specified period of time. The enzyme was denatured by placing the sample in an 80 °C oven for 10 min. After the guar solution and hydrogels were cooled, FITC-dextran probes were added, and the sample was placed on the Thermolyne RotaMixer for 24 h to ensure a homogeneous distribution. Aluminum foil was placed over the sample to prevent stray light from bleaching the FITC-dextran probes.

Diffusion Coefficient Measurements. The diffusion coefficient of FITC-dextran probes was quantified using the LSCM and the FRAP technique as previously mentioned.[23] A Leica TCS NT laser scanning confocal microscope with a 10 × 0.3NA dry PL Fluotar Objective, and an argon ion laser was used to perform the FRAP experiments. The 10 × 0.3NA dry PL Fluotar Objective was chosen to have a cylindrical bleaching volume, so that diffusion in the third dimension can be avoided. The FRAP experiment is summarized below. The LSCM scans an *xy* image of the sample at a specified location on the *z*-axis. The center of the incubation chamber (110 μm above the microscope slide) was chosen as the *z*-component for FRAP experiments. The *xy* image is referred to as the confocal plane, which means that only light emitted from this plane is detected by the photomultiplier tube (PMT) detector. A specified volume element was selected and bleached for 10 s with a high-intensity laser, followed by detection of the fluorescence recovery with a low-intensity laser. Unless otherwise specified, the fluorescence recovery of the bleached spot at 110 μm above the microscope slide (center of the sample) was recorded as a function of time. The fluorescence recovery was normalized by dividing the fluorescence intensity by that of the bleach spot prior to bleaching. The diffusion coefficient of the probe molecule can be obtained from the normalized fluorescence recovery curve ($f(t)$) based on the following theoretical equations as previously described by Blonk et al. (1993):[19]

$$f(t) = \sum_{n=0}^{n=\infty} \frac{(-k)^n}{n!} \frac{1}{1 + n[1 + (2t/\tau_D)]}$$

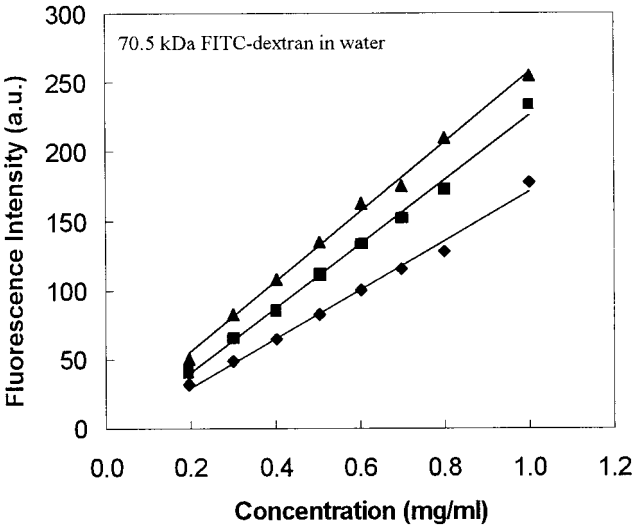

Figure 1. Dependence of the fluorescence intensity (arbitrary units) as a function of 70.5 kDa FITC-dextran probe concentration and photomultiplier tube detector (PMT) gain setting. The gain settings for the PMT were 481 (◆), 495 (■), and 506 (▲). The laser intensity (I) was 3% of I_{total}, and all trend lines had R^2 values higher than 0.99.

where k is a bleaching constant and is calculated using the equation

$$\frac{I(0)}{I(t<0)} = \frac{1 - e^{-k}}{k}$$

where $I(0)$ is the fluorescence intensity immediately after bleaching and $I(t<0)$ is the fluorescence intensity prior to bleaching. Finally, the diffusion coefficient is calculated from $D = \omega^2/4\tau_D$ where τ_D is the characteristic diffusion time and ω is the half-width at e^{-2} height of the Gaussian profile of the bleached spot intensity.[24]

When obtaining data using the LSCM, care was taken to avoid fluorescence saturation. Fluorescence saturation occurs when the exciting illumination is so intense that a significant fraction of the fluorophores is in the excited state and is no longer able to respond to the incident intensity. In our experiments, the intensity of the illuminating laser was kept below the saturation threshold of fluorescein by ascertaining that the emission was doubled when the illumination intensity was doubled. On the basis of the observation of linearity of emission with respect to illumination intensity, we believe that the phenomenon of saturation was not a problem in our imaging and quantification.

The depth at which diffusion measurements were taken was at the center of the sample, unless otherwise stated. When the depth of the diffusion measurement was varied, the height change of the stage was recorded and was referred to as the apparent depth. This is not the actual depth because the laser's focal plane is altered due to refractive index of the coverslip and the sample. The actual depth can be calculated with additional information on the refractive index of the coverslip and its thickness as well as the refractive index of guar. The refractive index of guar has not been reported in the literature, but it can be determined from the refractive index increment of guar ($dn/dc = 0.146$ mL/g).[25]

III. Results and Discussion

Linear Region of Fluorescence Intensity. Prior to the FRAP experiment, the correct laser intensity, photomultiplier tube detector setting, and fluorescent probe concentration must be determined. All three of these components contribute to the fluorescence intensity and must be considered to prevent saturation of the detector. Figure 1 shows the fluorescence intensity as a function of the PMT setting and the 70.5 kDa FITC-dextran probe concentration. The fluorescence intensity is linear for all PMT settings shown and for probe concentrations below 0.6 mg/mL. Above 0.6 mg/mL, the deviation from linearity is small, but it is unnecessary to use a concentration this high. A laser intensity of 3% of I_{total} was chosen for this set of data, yet it is important to be sure that this setting is not on the fringe of linearity. Therefore, Figure 2 presents the fluorescence intensity as a function of laser intensity. A laser intensity of 3% is well within the linear range. For all FRAP experiments, a 0.4 mg/mL probe concentration and a PMT setting of 481 were used with a laser intensity of 3% of I_{total} for recovery measurements.

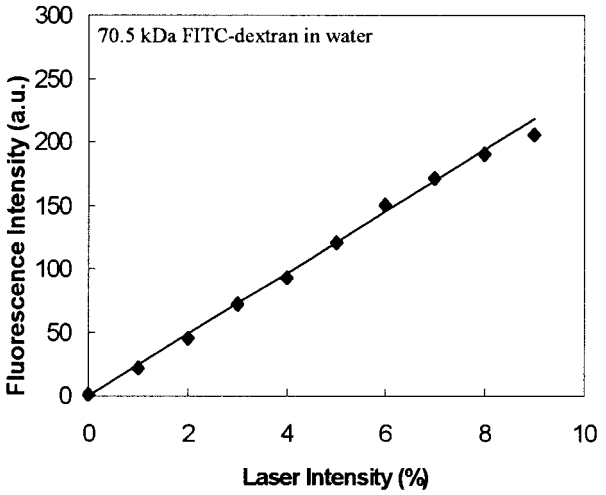

Figure 2. Fluorescence intensity in arbitrary units is presented as a function of the laser intensity for a 0.4 mg/mL 70.5 kDa FITC-dextran probe. The units for laser intensity (I) is presented as a percentage of the total intensity, I_{total}. The trend line had an R^2 value above 0.99 for laser intensities below 8% of I_{total}.

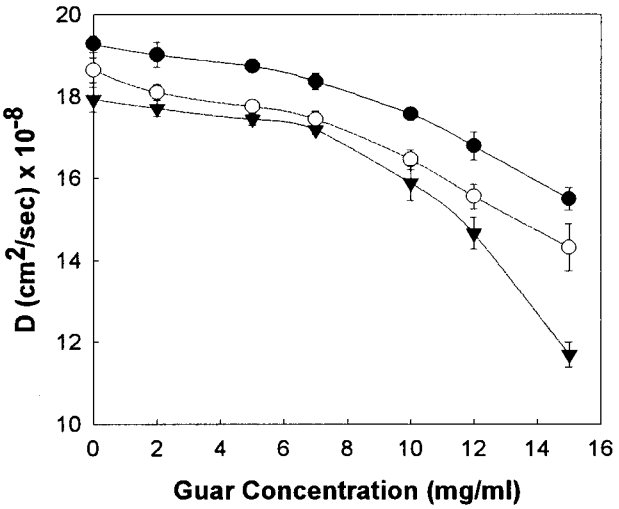

Figure 3. Diffusion coefficient of FITC-dextran probes in guar solutions, shown as a function of the guar concentration for three different molecular weights of FITC-dextran probes: 20 (●), 40 (○), and 70.5 kDa (▼).

Diffusion of FITC-Dextran Probes in Guar Solutions. At a specified temperature, the primary factors dictating the diffusion of the FITC-dextran probes are the concentration of the guar solution as well as the size of the probe. Figure 3 presents the diffusion coefficient as a function of guar concentration for three different

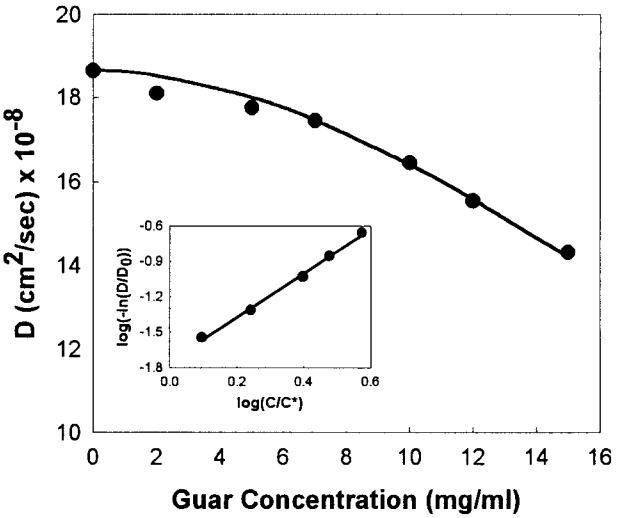

Figure 4. Experimental diffusion coefficient of 40 kDa FITC-dextran probe as a function of the guar concentration (●), including the predicted concentration dependence from the stretched-exponential equation: $D = 1.87 \times 10^{-7} \exp(-0.0231\text{-}(C/4)^{1.86})$ displayed as the solid line (—). The inset is a plot of the $\log[-\ln(D/D_0)]$ versus $\log(C/C^*)$, which was used to determine the parameters of the preceding equation.

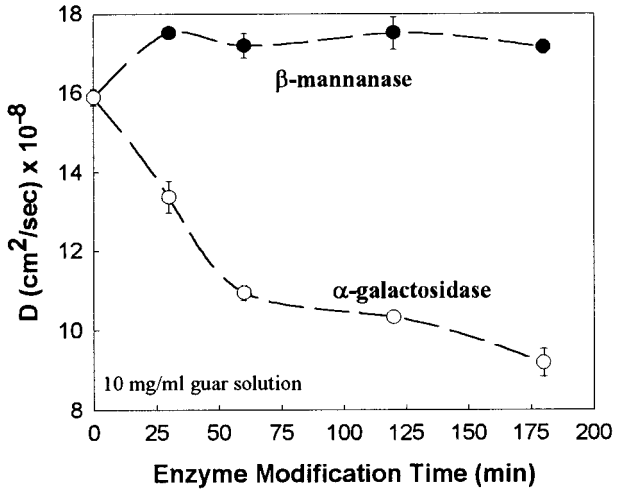

Figure 5. Diffusion coefficient of a 70.5 kDa FITC-dextran probe in an enzyme-modified 10 mg/mL guar solution as a function of the time incubated with β-mannanase (●) or α-galactosidase (○). The concentration of β-mannanase was 8.3×10^{-4} U/mL, and α-galactosidase was 8.3×10^{-3} U/mL.

molecular weight FITC-dextran probes. At low guar concentration, the diffusion coefficient only decreases slightly as guar concentration is increased. However, at higher guar concentrations there is a larger dependence on the concentration, suggesting a shift in the mode of diffusion. This phenomenon is normally attributed to the continuous change from infinite-dilution to Rouse to reptation dynamics.[26] According to scaling theory, the diffusion coefficient (D) has a power law dependence with concentration (C).[27] Unfortunately, log−log plots of D versus C did not yield a straight line. It is important to note that the power law dependency was developed for self-diffusion coefficients and can only correctly predict the diffusion when the probes and polymer molecular weight are similar.[28] Nonlinear log−log plots of D versus C have also been observed for other linear polymer probes in polysaccharide solutions.[26] An alternative equation that describes the diffusion in polymer solutions is the stretched-exponential form: $D = D_0 \exp(-aC^b)$, where D_0 is the diffusion coefficient in the pure solvent, C is the concentration of the polymer solution, a is a scaling prefactor, and b is the stretching exponent.[29] This equation has been further modified to take into account the chain overlap concentration by Phillies et al.[30] to become $D/D_0 = \exp(-a(C/C^*)^b)$. This modification allows the equation to be valid for all polymer concentration regimes. For guar solutions, the chain overlap concentration is inversely proportional to the intrinsic viscosity: $C^* \approx 4/[\eta]$.[8] The intrinsic viscosity has been previously determined in our laboratory to be 10 dL/g (or 1 mL/mg), yielding a chain overlap concentration of 4 mg/mL.[4] Using this value of C^*, we observed a good correlation between the experimental data of Figure 3 and the stretched-exponential form. This is illustrated in Figure 4 for the 40 kDa FITC-dextran probe. A straight line is observed when $\log[-\ln(D/D_0)]$ is plotted versus $\log(C/C^*)$ as shown in the inset of Figure 4. The value of D_0 was experimentally determined to be 1.87×10^{-7} cm²/s; the values of a and b were calculated from the slope and intercept of the inset in Figure 4 and found to be −0.0231 and 1.8639, respectively. When these parameters are input into the stretched-exponential form, the model predicts the diffusion coefficient versus guar concentration data very well as shown in Figure 4 for the 40 kDa FITC-dextran probe. However, it is important to note that when obtaining the constants for the stretched-exponential equation, the observed linearity only occurred at concentrations at or above the chain overlap concentration. This type of diffusion-polymer concentration dependence has been previously observed for poly(ethylene oxide) diffusing in ethyl(hydroxyethyl)cellulose when attempting to fit the stretched-exponential form to experimental data.[26] One unique feature of ethyl(hydroxyethyl)-cellulose and guar galactomannan versus most polymers is their ability to self-aggregate. This occurs where segments of the polysaccharide backbone are unbranched, and intermolecular hydrogen bonding is present.[8,31] This may play a role in the observed nonlinearity below the chain overlap concentration. The stretched-exponential form has not met with universal acceptance, although it has proven to be extremely successful in describing the concentration dependence of D and allows interpolation of data to particular concentration regimes.[32] This model emphasizes intermolecular hydrodynamic interactions over topological constraints, which is in contrast to other models such as reptation plus scaling, modified reptation models, and cooperative chain motion models.[33]

Diffusion in Enzyme Modified Guar Solutions. The diffusion coefficient of a 70.5 kDa FITC-dextran probe was studied in 10 mg/mL guar solutions treated with either β-mannanase or α-galactosidase. Enzyme treatment of guar solutions with backbone cleaving β-mannanase is known to reduce the viscosity.[34−36] According to the Stokes−Einstein equation, the diffusion coefficient is inversely proportional to the viscosity.[29] Therefore, β-mannanase treatment of guar solutions should increase the diffusion coefficient, which agrees with our results shown in Figure 5. After only 30 min of enzyme treatment with 8.3×10^{-4} U/mL β-mannanase, the diffusion coefficient of the 70.5 kDa FITC-dextran probe increases to that of its diffusion coefficient in water. However, the diffusion coefficient of α-galactosidase (a side chain cleaving enzyme)-treated guar solution shows an opposite trend (Figure 5). Initially, the diffusion coefficient decreases rapidly

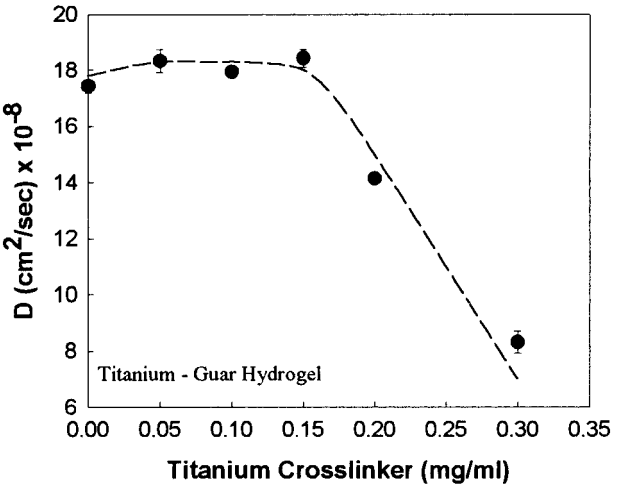

Figure 6. Diffusion coefficient of a 70.5 kDa FITC-dextran probe as a function of titanium cross-linker (mg/mL) used to cross-link a 5 mg/mL guar solution.

followed by a slow decrease at longer times. To understand the decline in the diffusion coefficient upon α-galactosidase treatment, we need to consider how the fine structure of guar has changed. Guar is unique among biopolymers due to the "hyperentanglements" which are formed between guar molecules.[37] "Hyperentanglements" occur through intermolecular aggregation of portions of the guar molecule that lack galactose branches. The mannan backbone aggregates due to intermolecular hydrogen bonding of cis hydroxyls on mannose. Therefore, α-galactosidase treatment of guar solutions creates additional "hyperentanglements", or cross-links, which results in a reduction of the diffusion coefficient. If this hypothesis is correct, a similar trend should be observed for the diffusion coefficient of a cross-linked guar hydrogel.

Diffusion in Guar-Titanium Hydrogels. The diffusion coefficient of a 70.5 kDa FITC-dextran probe was studied for a 0.5 mg/mL guar solution cross-linked with 0−0.3 mg/mL of titanium. The diffusion coefficient as a function of titanium cross-linker concentration is shown in Figure 6. For lightly cross-linked guar solutions (titanium concentration below 0.15 mg/mL), the diffusion coefficient is not affected by cross-linking. However, above 0.15 mg/mL titanium the diffusion coefficient decreases rapidly because of the formation of additional cross-links analogous to those formed by the "hyperentanglements". These additional cross-links do not simply bind closely spaced guar molecules but must alter the structure of the hydrogel to create a denser network.

Diffusion in Enzyme-Modified Guar-Titanium Hydrogels. Guar-titanium hydrogels were prepared at a concentration of 5 and 0.2 mg/mL of guar and titanium, respectively. The diffusion coefficient of a 70.5 kDa FITC-dextran probe was studied after enzyme treatment with either 0.166 U/mL β-mannanase or 1.66 U/mL α-galactosidase for specified amounts of time. This is illustrated in Figure 7, which shows the diffusion coefficient as a function of enzyme modification time. We find the diffusion coefficient in guar-titanium hydrogels treated with β-mannanase to follow the same trend as the guar solution; the diffusion coefficient increases to the probe diffusion coefficient in water after approximately 3 h of enzyme treatment. For the α-galactosidase-treated hydrogels, we observe some unique features in the diffusion coefficient as a function of

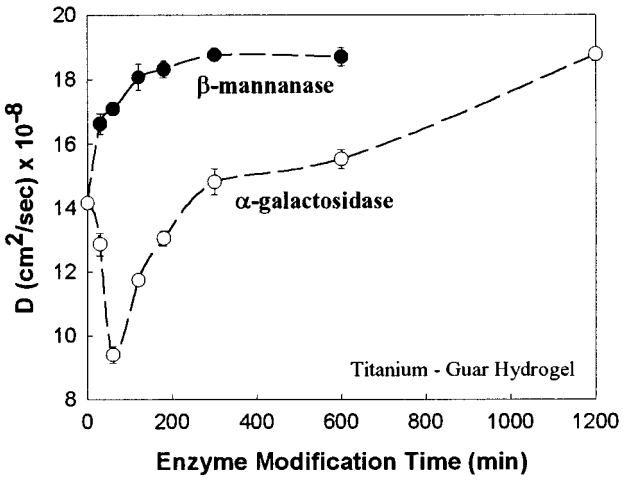

Figure 7. Diffusion coefficient of a 70.5 kDa FITC-dextran probe in an enzyme-modified guar hydrogel as a function of time incubated with β-mannanase (●) or α-galactosidase (○). The concentration of β-mannanase was 0.166 U/mL, and α-galactosidase was 1.66 U/mL. The hydrogel had a titanium cross-linker concentration of 0.2 mg/mL and a guar concentration of 5 mg/mL.

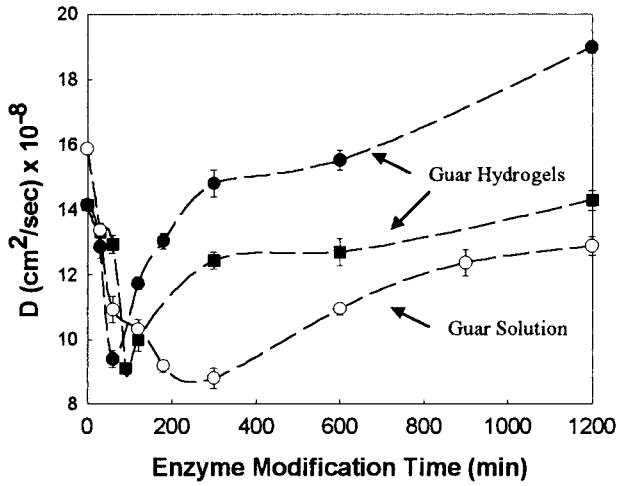

Figure 8. Diffusion coefficient of a 70.5 kDa FITC-dextran probe in titanium cross-linked guar hydrogel (5 mg/mL guar−0.2 mg/mL titanium) and guar solution (10 mg/mL), as a function of time incubated with α-galactosidase. Results are shown for two different enzyme concentrations in the hydrogels, 1.66 (●) and 0.83 U/mL (■), and one enzyme concentration in the guar solution, 8.3×10^{-3} U/mL (○).

enzyme modification time. After an initial trend of a decreasing diffusion coefficient, there is a rapid increase in the diffusion coefficient followed by a slow increase to approximately the probe diffusion coefficient in water.

The counterintuitive result of the diffusion coefficient behavior for the α-galactosidase-treated hydrogels led to further investigation of α-galactosidase-treated guar solutions at longer enzyme modification times and of α-galactosidase-treated hydrogels at different enzyme concentrations. These results are illustrated in Figure 8. The unique diffusion coefficient behavior in Figure 7 is found to be present not only in guar-titanium hydrogels but also in guar solutions, albeit, the rate of change of the diffusion coefficient is smaller. All of the α-galactosidase-treated samples show a minimum value for the diffusion coefficient of $\sim 9.0 \times 10^{-8}$ cm^2/s. One explanation for the upturn in the diffusion coefficient is the occurrence of phase separation due to the additional intermolecular cross-links ("hyperentangle-

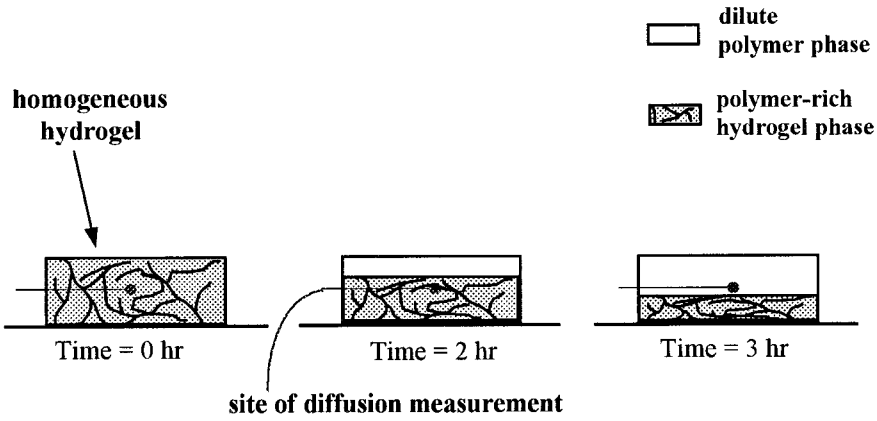

Figure 9. Pictorial representation of the precipitation/phase separation behavior of guar-based systems. When the amount of cross-links are too high to maintain a homogeneous system, phase separation produces a dilute polymer phase and a polymer-rich hydrogel phase. As cross-linking continues to increase, the polymer-rich hydrogel phase collapses into a dense network, which can fall below the site of diffusion coefficient measurements.

ments") created by the removal of the galactose branches. It is known that increasing the cross-links of guar hydrogels reduces the degree of swelling (i.e., the water holding capacity).[38] It has also been observed that guar solutions cross-linked with Borax ions phase separate as the number of cross-links per chain reaches a critical level.[39] This results in an expulsion of water from the hydrogel to form a dilute polymer phase and a polymer-rich hydrogel phase. The laser scanning confocal microscope only scans one *xy*-plane in the sample, and we choose a *z*-coordinate at the center of the sample. If phase separation is occurring, the hydrogel would collapse upon itself and the hydrogel volume would decrease, thus causing an increase in the diffusion coefficient. As this continues, the majority of the hydrogel would fall below the height of the *xy*-plane scanned by the LSCM. In this case, the LSCM would be measuring the diffusion coefficient in the dilute polymer phase. A pictorial representation of this hypothesis is shown in Figure 9. As α-galactosidase continues to remove galactose branches from the guar molecules, the guar in the dilute polymer phase would eventually fall out of solution, and the diffusion coefficient of the probes in water will be measured. This assumes that the FITC-dextran probe is present in both the dilute polymer and the hydrogel phase. To determine whether the additional cross-links were the reason for phase separation, guar-titanium gels were created with higher titanium cross-linker concentrations. Figure 10 shows the diffusion coefficient in titanium cross-linked hydrogels as a function of titanium concentration. If phase separation is only dependent on the number of cross-links per guar molecule, it should yield the same results whether the cross-links are formed by titanium or α-galactosidase treatment. As shown in Figure 10, as the titanium cross-linker concentration is increased, the same behavior of the diffusion coefficient is observed, with a minimum diffusion coefficient occurring at $\sim 8 \times 10^{-8}$ to 9×10^{-8} cm^2/s. The inset in Figure 10 shows that this trend is not dependent on the size of the FITC-dextran probe.

Scanning Depth in the Phase-Separated System. Since the LSCM only measures the diffusion coefficient at a particular depth in the sample, it is possible to obtain the diffusion coefficient in the hydrogel and liquid portion of the phase-separated system by adjusting the scanning depth. The diffusion coefficient remained independent of the scanning depth until at least 2 h of

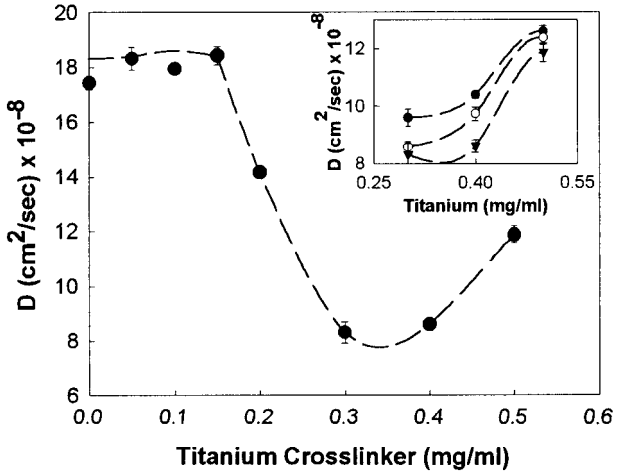

Figure 10. Diffusion coefficient of a 70.5 kDa FITC-dextran probe as a function of titanium cross-linker used to cross-link a 0.5 mg/mL guar solution. The inset plot shows that the diffusion coefficient increases for all molecular weight probes when the cross-linker concentration is increased from 0.3 to 0.5 mg/mL titanium: 20 (●), 40 (○), and 70.5 kDa (▼).

α-galactosidase incubation (data not presented). Therefore, the effect of apparent scanning depth on the diffusion coefficient for a α-galactosidase-treated guar-titanium gel treated for 3 h is shown in Figure 11. From Figure 11, we find that as the apparent scanning depth is changed from the center of the sample, there is an initial plateau region where the diffusion coefficient is approximately 1.3×10^{-7} cm^2/s. At 20 μm below the center, the diffusion coefficient begins to decrease until a second lower plateau region is reached at 50 μm with a diffusion coefficient of approximately 6.0×10^{-8} cm^2/s. The two plateau regions correspond to the two phases: the dilute polymer phase and the polymer-rich hydrogel phase. By changing the apparent scanning depth to the second lower plateau region, the diffusion coefficient specifically in the hydrogel phase can be measured. Thus, our experimental approach using confocal microscopy, in addition to providing the diffusion coefficient, offers a powerful tool to probe the homogeneity of material microstructure. It enables us to quantify the point of phase separation and gives us the ability to continue measuring diffusion coefficients in a phase-separated hydrogel. Such information has direct implication in many applications as in development of food additives using enzyme-modified guar.

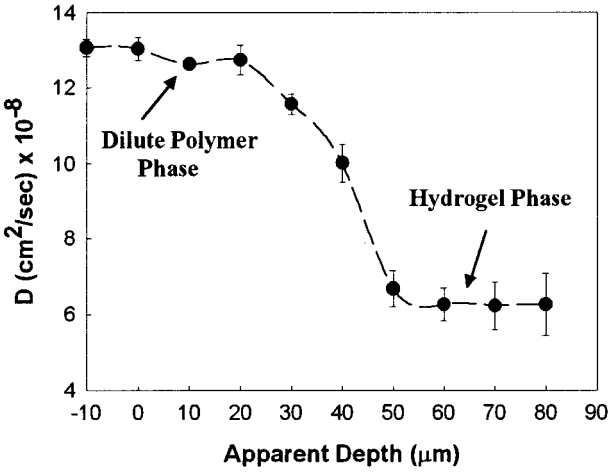

Figure 11. Diffusion coefficient of a 70.5 kDa FITC-dextran probe as a function of apparent depth below the center of the sample for a 5 mg/mL guar−0.2 mg/mL titanium hydrogel treated for 3 h with α-galactosidase at a concentration of 1.66 U/mL. A depth of 0 μm corresponds to the center of the sample, and as the depth increases the diffusion coefficient is measured at a lower position in the sample. By varying the apparent depth at which the diffusion coefficient is measured, a distinction between the dilute polymer phase and the hydrogel phase is observed.

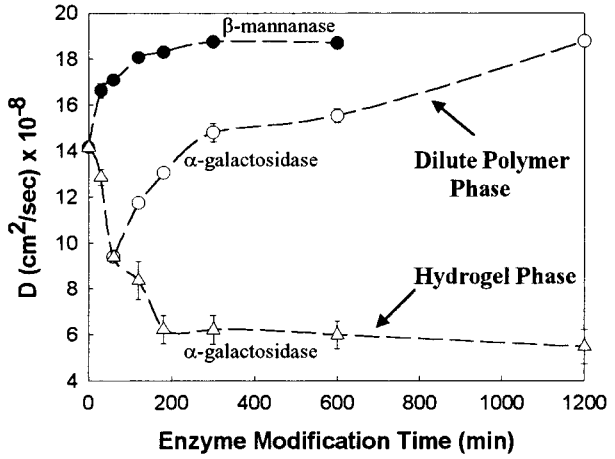

Figure 12. Diffusion coefficient of a 70.5 kDa FITC-dextran probe as a function of enzyme incubation time in a 5 mg/mL guar−0.2 mg/mL titanium hydrogel. β-Mannanase-treated guar hydrogels (●) remained as a one-phase system; however, α-galactosidase-treated guar hydrogels phase separated, and the diffusion coefficients in the dilute polymer phase (○) as well as the hydrogel phase (△) were both obtained. The concentration of β-mannanase was 0.166 U/mL, and α-galactosidase was 1.66 U/mL.

Figure 12 summarizes the effect of the enzyme treatment on guar-titanium gels by presenting the diffusion coefficient in both phases of the α-galactosidase-treated sample as well as the β-mannanase-treated sample. For the phase-separated α-galactosidase-treated samples, the diffusion coefficient in the hydrogel phase rapidly decreases until it reaches a value of approximately 6.0×10^{-8} cm^2/s, at 3 h of incubation. Further incubation with α-galactosidase only produces a limited decrease in the diffusion coefficient.

IV. Conclusions

In this study, we used laser scanning confocal microscopy combined with fluorescence recovery after photobleaching to measure the diffusion coefficient of macromolecules in enzymatically degraded guar solutions and hydrogels. It is clear that β-mannanase treatment of guar systems increases the diffusion coefficient; however, α-galactosidase treatment causes the precipitation of guar due to the formation of additional cross-links via "hyperentanglements" and results in a phase-separated system. The diffusion coefficients in α-galactosidase-treated guar solutions and hydrogel exhibit an initial sharp decrease to a value of approximately 9×10^{-8} cm^2/s. At this point, phase separation occurs and the diffusion coefficient in the dilute polymer phase increases until finally reaching the value of that in water, while the diffusion coefficient in polymer-rich hydrogel phase continues to decrease to a value of approximately 6×10^{-8} cm^2/s. The phase separation behavior observed in our study is consistent with the behavior found in highly cross-linked borax-guar hydrogels.

Acknowledgment. The authors gratefully acknowledge the National Science Foundation and the United States Department of Agriculture for financial support of this work.

References and Notes

(1) Tombs, M.; Harding, S. E. *An Introduction to Polysaccharide Biotechnology*; Taylor and Francis: New York, 1998.
(2) Daniel, J.; Whistler, R. In *Cereal Polysaccharides in Technology and Nutrition*; Rasper, V. F., Ed.; 1984; pp159−184.
(3) Bayerlein, F. In *Plant Polymeric Carbohydrates*; Meuser, F., Manners, D. J., Seibel, W., Eds.; 1993; pp 191−202.
(4) Tayal, A.; Pai, V.; Khan, S. A. *Macromolecules* **1999**, *32*, 5567−5574.
(5) Chidwick, H.; Dey, P.; Hart, R.; MacKenzie, A.; Pridham, J. *Biochem. Soc. Trans.* **1991**, *19*, 269.
(6) Launay, B.; Cuvelier, G.; Martinez-Reyes, S. *Carbohydr. Polym.* **1997**, *34*, 385−395.
(7) McCleary, B. V.; Clark, A. H.; Dea, I. C. M.; Rees, D. A. *Carbohydr. Res.* **1985**, *139*, 237−260.
(8) Robinson, G.; Ross-Murphy, S. B.; Morris, E. R. *Carbohydr. Res.* **1982**, *107*, 17−32.
(9) Kelly, R. M.; Khan, S. A.; Leduc, P.; Tayal, A.; Prud'homme, R. K. U.S. Patent # 5,421,412, 1995.
(10) Hirsch, S.; Binder, V.; Schehlmann, V.; Kolter, K.; Bauer, K. *Eur. J. Pharm. Biopharm.* **1999**, *47*, 61−71.
(11) Kloek, W.; Luyten, H.; vanVliet, T. *Food Hydrocolloids* **1996**, *10*, 123−129.
(12) Garnier, C.; Bouchet, B.; Gallant, D. J.; Doublier, J. L. *Sci. Aliments* **1999**, *19*, 459−470.
(13) Scherbukhin, V. D., Anulov, O. V. *Appl. Biochem. Microbiol.* **1999**, *35*, 229−244.
(14) McCleary, B. V.; Matheson, N. K. *Phytochemistry* **1976**, *15*, 43−47.
(15) Tayal, A.; Pai, V.; Kelly, R. M.; Khan, S. A. In *Water Soluble Polymers*; Plenum Press: New York, 1998; pp 41−49.
(16) Allaerts, W.; Engelborghs, Y.; Van Oostveldt, P.; Denef, C. *Endocrinology* **1990**, *127*, 1517−1525.
(17) Paddock, S. W. *Methods Mol. Biol.* **1999**, *122*, 1−9.
(18) Cutts, L. S.; Roberts, P. A.; Adler, J.; Davies, M. C.; Melia, C. D. *J. Microsc.* **1995**, *180*, 131−139.
(19) Blonk, J. C. G.; Don, A.; Van Aalst, H.; Birmingham, J. J. *J. Microsc.* **1993**, *169*, 363−374.
(20) Furukawa, R.; Arauzlara, J. L.; Ware, B. R. *Macromolecules* **1991**, *24*, 599−605.
(21) Bu, Z.; Russo, P. S. *Macromolecules* **1994**, *27*, 1187−1194.
(22) Westrin, B. A.; Axelsson, A.; Zacchi, G. *J. Controlled Release* **1994**, *30*, 189−199.
(23) De Smedt, S. C.; et al. *Macromolecules* **1997**, *30*, 4863−4870.
(24) Axelrod, D.; Koppel, D. E.; Schlessinger, J.; Elson, E.; Webb, W. W. *Biophys. J.* **1976**, *16*, 1055−1069.
(25) Beer, M. U.; Wood, P. J.; Weisz, J. *Carbohydr. Polym.* **1999**, *39*, 377−380.
(26) Nydén, M.; Söderman, O. *Macromolecules* **1998**, *31*, 4990−5002.
(27) Phillies, G. D. J.; et al. *Macromolecules* **1989**, *22*, 4068−4075.

(28) de Gennes, P.-G. *Scaling Concepts in Polymer Physics*; Cornell University Press: Ithaca, NY, 1979.
(29) De Smedt, S. C.; Meyvis, T. K. L.; Demeester, J. *Macromolecules* **1997**, *30*, 4863−4870.
(30) Philiies, G. D. J.; Brown, W.; Zhou, P. *Macromolecules* **1992**, *25*, 4948−4954.
(31) Nydén, M.; Söderman, O.; Karlström, G. *Macromolecules* **1999**, *32*, 127−135.
(32) Lodge, T. P.; Markland, P.; Wheeler, L. M. *Macromolecules* **1989**, *22*, 3409−3418.
(33) Wheeler, L. M.; Lodge, T. P. *Macromolecules* **1989**, *22*, 3399−3408.
(34) McCleary, B. V. *Methods Enzymol.* **1988**, *160*, 596−610.
(35) Tayal, A.; Kelly, R. M.; Khan, S. A. *Soc. Pet. Eng. J.* **1997**, *2*, 204.
(36) Tayal, A.; Kelly, R. M.; Khan, S. A. *Macromolecules* **1999**, *32*, 294−300.
(37) Dea, I. C. M.; Morrison, A. *Adv. Carbohydr. Chem. Biochem.* **1975**, *31*, 241−312.
(38) Gliko-Kabir, I.; Yagen, B.; Penhasi, A.; Rubinstein, A. *Pharm. Res.* **1998**, *15*, 1019−1025.
(39) Pezron, E.; Leibler, L.; Ricard, A.; Audebert, R. *Macromolecules* **1988**, *21*, 1126−1131.

MA000786L